npg

ORIGINAL ARTICLE

Antileukemic activity of the HSP70 inhibitor pifithrin-μ in acute leukemia

M Kaiser[1,3], A Kühnl[1,3], J Reins[1], S Fischer[1], J Ortiz-Tanchez[1], C Schlee[1], LH Mochmann[1], S Heesch[1], O Benlasfer[1], W-K Hofmann[2], E Thiel[1] and CD Baldus[1]

[1]Department of Hematology and Oncology, Charité University Hospital, Campus Benjamin Franklin, Berlin, Germany and [2]Department of Hematology and Oncology, University Hospital Mannheim, Mannheim, Germany

Heat shock protein (HSP) 70 is aberrantly expressed in different malignancies and has emerged as a promising new target for anticancer therapy. Here, we analyzed the *in vitro* antileukemic effects of pifithrin-μ (PFT-μ), an inhibitor of inducible HSP70, in acute myeloid leukemia (AML) and acute lymphoblastic leukemia (ALL) cell lines, as well as in primary AML blasts. PFT-μ significantly inhibited cell viability at low micromolar concentrations in all cell lines tested, with IC50 values ranging from 2.5 to 12.7 μM, and was highly active in primary AML blasts with a median IC50 of 8.9 μM (range 5.7–37.2). Importantly, higher IC50 values were seen in normal hematopoietic cells. In AML and ALL, PFT-μ induced apoptosis and cell cycle arrest in a dose-dependent fashion. PFT-μ also led to an increase of the active form of caspase-3 and reduced the intracellular concentrations of AKT and ERK1/2 in NALM-6 cells. Moreover, PFT-μ enhanced cytotoxicity of cytarabine, 17-(allylamino)-17-desmethoxygeldanamycin, suberoylanilide hydroxamic acid, and sorafenib in NALM-6, TOM-1 and KG-1a cells. This is the first study demonstrating significant antileukemic effects of the HSP70 inhibitor PFT-μ, alone and in combination with different antineoplastic drugs in both AML and ALL. Our results suggest a potential therapeutic role for PFT-μ in acute leukemias.

Introduction

Despite risk-adapted treatment strategies, only about 35% of adult patients with acute myeloid leukemia (AML) under 60 years of age can be cured.[1] Equally, in acute lymphoblastic leukemia (ALL), outcome of adult patients remains poor, with a long-term survival of 30–50%.[2] Further dose intensification of chemotherapeutic agents showed limited antileukemic efficacy and high toxicity, with an increased risk of early deaths. Therefore, efforts have been made to develop new molecular therapies for combination treatment with classic chemotherapies. In *BCR-ABL* positive ALL, outcome has considerably improved with the introduction of imatinib mesylate.[3] Similarly in AML, different molecular drugs like FLT3 inhibitors,[4] proteasome inhibitors,[5] histone deacetylase inhibitors[6] or heat shock protein (HSP) 90 inhibitors[7] are currently under preclinical and clinical investigations.

Besides HSP90, also HSP70, the second major HSP, has been identified as a promising target for antileukemic therapy. HSP70 (also termed HSP72) constitutes the inducible cytosolic isoform of the human HSP70 family that consists of at least eight different members.[8] HSP70 is an ATP-dependent chaperone that is induced by cellular stress and protects cells against various apoptotic stimuli. HSP70 mainly acts as stabilizer of multi-protein complexes and prevents the intracellular accumulation of misfolded or damaged proteins.[9]

Although in normal unstressed cells the expression of HSP70 is very low, aberrant overexpression of HSP70 is observed in many solid and hematologic tumors.[10] In different carcinomas, high expression of HSP70 has been correlated with poor outcome.[11,12] In AML, overexpression of HSP70 mRNA has been associated with a lower complete remission rate and inferior overall survival.[13] High expression of cell-surface HSP70 and high serum levels of circulating HSP70 were associated with shorter survival in AML patients.[14,15] These clinical findings are confirmed by *in vitro* and *in vivo* studies that suggest an active role of HSP70 in tumorigenicity[16–18] and chemoresistance.[19] Accordingly, reduction of HSP70 levels induced cell death in different cancer cell lines[20–22] and sensitized tumor cells to antineoplastic agents.[23,24] In leukemic cells, HSP70 has an important role in cell cycle control, survival and inhibition of caspase-dependent and -independent apoptosis.[25,26] In particular, upregulation of HSP70 has been shown to confer drug resistance in AML and chronic myeloid leukemia cells.[27,28] Conversely, depletion of HSP70 by small interfering RNA enhanced the antileukemic activity of the HSP90 inhibitor 17-(allylamino)-17-desmethoxygeldanamycin (17-AAG).[29]

Because of its prognostic implications and functional role in acute leukemias, HSP70 represents an interesting target for antileukemic therapy. However, the design of selective pharmacological inhibitors of HSP70 has been difficult and only few have been described so far.[30] Recently, the small molecule pifithrin-μ (PFT-μ) was identified as a specific inhibitor of inducible HSP70.[31] PFT-μ interferes with the carboxyterminal substrate-binding domain of inducible HSP70 and disrupts its association with client proteins. Here, we have evaluated *in vitro* effects of PFT-μ in acute leukemia cell lines and in primary AML blasts and found a remarkable antileukemic potential of this inhibitor.

Materials and methods

Cell lines and cell culture
The human cell lines KG-1a (AML), NALM-6 (B-precursor ALL), TOM-1 (B-precursor ALL; *BCR-ABL* positive), Jurkat, BE-13 (both T-cell leukemia) and K562 (chronic myeloid leukemia, blast crisis) were obtained from the DSMZ (Braunschweig, Germany) and cultured as recommended. The cytarabine-resistant K562

2

cell line was generated by continuous exposure of K562 cells over several passages to subsequently increasing concentrations of cytarabine (0.5 to 256 ng/ml).

Patient samples

Primary human bone marrow (BM) leukemic blasts were obtained from patients with newly diagnosed or relapsed AML with sufficient material available. Morphological and genetic diagnostic analyses were performed in the institutional laboratories.

BM leukemia blasts were separated using density gradient centrifugation with Ficoll-Hypaque (Amersham Pharmacia Biotech, Uppsala, Sweden). Cells were resuspended in RPMI 1640 supplemented with 20% fetal calf serum, and immediately seeded in 96-well plates for experimental procedures. Peripheral blood (PB) mononuclear cells (MNC) and CD34-positive hematopoietic progenitor cells were collected from healthy donors, as described previously.[32] MNC were directly resuspended in RPMI 1640 with 20% fetal calf serum and incubated with PFT-µ for further analyses. Selected CD34-positive cells were suspended in RPMI 1640 (20% fetal calf serum), with the addition of 50 ng/ml stem cell factor and 20 ng/ml interleukin-3 (both from Miltenyi Biotech, Bergisch Gladbach, Germany). Cells were cultivated for 48 h before being seeded in 96-well culture plates. Human BM mesenchymal stromal cells (BMSC) were isolated by plastic adherence as previously described,[33] and early passages were used for further analyses. Because of the BMSCs' lower proliferation rate, cells were exposed to PFT-µ for 72 h instead of 48 h for viability assays.

Informed consent was obtained from all patients and donors, and the study was conducted with approval of the local ethics committee and in accordance with the Declaration of Helsinki.

Reagents

Pifithrin-µ (2-phenylethynesulfonamide; Merck Chemicals, Darmstadt, Germany), 17-AAG, suberoylanilide hydroxamic acid (SAHA) and sorafenib (BAY 43-9006; all from Alexis/Enzo Life Sciences, Loerrach, Germany) were dissolved in dimethyl sulfoxide and stored at $-80\,°C$. Cytarabine (Merck Chemicals) was freshly dissolved in water and stored for limited time intervals at $4\,°C$. Pan caspase inhibitor Z-VAD-FMK (BD Biosciences, Heidelberg, Germany) was dissolved in dimethyl sulfoxide and stored at $-20\,°C$.

Viability assays

Changes in cell viability were determined using the colorimetric WST-1 (2-[4-Iodophenyl]-3-[4-nitrophenyl]-5-[2,4-disulfophenyl]-2H-tetrazolium; Roche Diagnostics, Mannheim, Germany) assay. Briefly, cells were plated in 96-well plates in quadruplicates. Cell lines were allowed to proliferate for 24 h to reach exponential growth rates. Subsequently, PFT-µ, 17-AAG, cytarabine, SAHA or sorafenib were added at different concentrations, either as single substance or in combination. In order to determine additive effects in combination experiments, substances were added at sub-apoptotic concentrations simultaneously for 48 h. In addition, SAHA was also tested with 24 h of pre-incubation time as a single substance, before PFT-µ was added for additional 48 h of co-incubation. For experiments with PB MNC or primary leukemia blasts, PFT-µ was added immediately to cells after sample preparation. Cells were then incubated for 48–72 h at cell culture conditions and proliferation assays were performed according to the manufacturer's

protocol. Chemical reduction of the WST-1 dye was determined by optical density absorption analyses at 450 nm, using an ELISA plate reader (Dynatech International, Chantilly, VA, USA).

Cell cycle and apoptosis assays

Cell lines NALM-6 and KG-1a were cultured until reaching exponential growth phase and were incubated in the presence of PFT-µ for additional 24 h. Subsequently, bromodeoxyuridine (BrdU) was added for the final 2 h of incubation. Cells were resuspended in Cytofix/Cytoperm buffer (BD Biosciences), stained with anti-BrdU FITC-conjugated monoclonal antibodies (BD Biosciences) and 7-aminoactinomycin D (7-AAD) for the determination of total DNA levels. Cells were analyzed by flow cytometry (BD Biosciences) and data analysis was performed using CellQuest Pro software (BD Biosciences). Cells were gated for intact cell material by forward/sideward scatter properties, and populations representing subG0/1, G0/1, S and G2/M phases were identified and quantified by their individual BrdU/ 7-AAD staining pattern. At least two independent sets of experiments were performed for each cell line.

For detection of apoptosis, cells were incubated in the presence of PFT-µ for 48 h. Subsequently, cells were stained for Annexin V using the Annexin V-FITC/7-AAD apoptosis detection kit (BD Biosciences) following the manufacturer's instructions. Specific apoptosis was calculated as described before.[34]

Caspase-3 activity assay

After reaching exponential growth rates, NALM-6 and KG-1a were incubated with PFT-µ for 24 h. Active caspase-3 was analyzed by flow cytometry, using an anti-active-caspase-3 PE antibody (BD Biosciences) after cells were fixed and permeabilized.

Staining of intracellular proteins

NALM-6 cells in exponential growth phase were incubated with $10\,\mu M$ PFT-µ for 10 h under regular cell culture conditions. Afterwards, cells were fixed with Fix Buffer I (BD Biosciences) and permeabilized with methanol. Target proteins were stained using antibodies against AKT (#9272), p-AKT (Ser473) (#4058), ERK1/2 (#9102; all from Cell Signaling Technology, Danvers, MA, USA), p-ERK1/2 (T202/Y204), (612593; BD Biosciences) and HSP70 (GTX23148; GeneTex, Irvine, CA, USA). Except for p-ERK1/2, which is a primary Alexa Fluor 647 conjugated antibody, incubations with primary antibodies were followed by staining with Alexa Fluor 647 goat anti-rabbit antibody (A21244; Invitrogen, Karlsruhe, Germany). Corresponding isotype antibody controls were performed for each experiment. Cells were analyzed by flow cytometry and gated for the live cell population defined in forward/sideward scatter plots. Data were analyzed using Flowjo software (Tree Star, Ashland, OR, USA). Shifts in median fluorescence value (MFV) of treated samples versus the corresponding controls were analyzed, and MFVs of untreated controls were defined as 100%. Shifts in MFVs of more than 25% in the treatment group in relation to untreated controls were considered as increases or decreases in intracellular protein concentrations. MFV of isotype controls of untreated and treated cells were virtually unaffected (MFV shifts $<10\%$).

Statistical analysis

Non-parametric statistics (Mann–Whitney U-test) were performed using SPSS Version 18.0 software (SPSS Software, Munich, Germany). P-values <0.05 were regarded significant.

Results

PFT-µ inhibits proliferation of leukemic cell lines and primary blasts

Leukemic cell lines and primary cells from AML patients were exposed to different concentrations of PFT-µ (0.5 to 100 µM) for 48 h. PFT-µ induced a dose-dependent inhibition of proliferation in all cell samples tested (Table 1 and Figure 1). In leukemic cell lines, incubation with PFT-µ strongly inhibited viability, with IC50 values ranging from 2.5 to 12.7 µM (Table 1). PFT-µ of 50 µM led to a complete abrogation of viability in all cell lines tested. Interestingly, the least sensitive cell line KG-1a revealed a particularly low basal HSP70 expression as determined by intracellular fluorescence-activated cell sorting analysis. However, no significant association between basal HSP70 levels and IC50 values were observed in the different leukemic cell lines. In primary AML blasts, IC50 values ranged from 5.7 to 37.2 µM (median 8.9 µM), with a maximum inhibition of 79 to 100% (Table 1). The lowest sensitivity to PFT-µ was observed in a sample derived from a patient with *FLT3*-internal tandem duplication; however, no statistically significant associations between patients' clinical or genetic features and IC50 values were found. Notably, no difference was seen between pretreatment samples and relapsed patients regarding IC50 values in the small number of patient samples tested (Table 1).

To evaluate cytotoxicity of PFT-µ in non-malignant cells, we analyzed BMSC samples of four AML patients, as well as PB MNC ($n = 6$) and CD34-positive cell samples ($n = 5$) from healthy donors. In one BMSC sample, IC50 value was not reached with 100 µM PFT-µ. The remaining three BMSC samples showed a median IC50 value of 37.7 µM (range 36.3–44.1). Median IC50 values in PB MNC and CD34-positive cells were 17.6 µM (range 10.4–42.3) and 15.1 µM (range 8.0–20.0), respectively, suggesting

a higher resistance of normal hematopoietic and stromal cells to PFT-µ, as compared with leukemic blasts.

PFT-µ induces cell cycle arrest and apoptosis in leukemic cells

To further evaluate the impact of PFT-µ on leukemic cells, we performed cell cycle and apoptosis analyses with the cell lines NALM-6 and KG-1a. Cell cycle analyses using BrdU/7-AAD staining revealed a markedly reduced proportion of cells in S phase after 24 h incubation, with PFT-µ at concentrations of 4 and 5 µM for NALM-6, and 40 and 60 µM for KG-1a (Figure 2a). NALM-6 cells shifted equally to G0/1 and G2/M phases, KG-1a mainly entered G2/M phase arrest (Figure 2a). Interestingly,
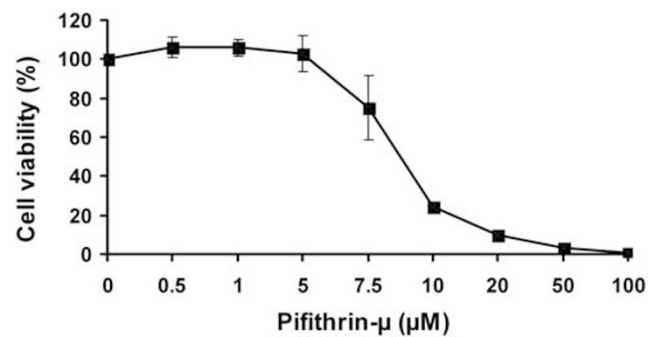

Figure 1 Dose-dependent inhibition of proliferation of primary AML cells by PFT-µ. A representative figure is shown (patient no. 5). Cells were incubated with different concentrations of PFT-µ for 48 h and viability was measured by WST-1 assay. Data are presented as the mean value of four replicates. Error bars indicate standard error.

Table 1 IC50 and maximum inhibition values of PFT-µ in leukemic cell lines and primary cells derived from AML patients

Cell line	Characteristics					IC50 (µM)	Max. inhib. (%)
NALM-6	B-precursor ALL					2.5	100
TOM-1	B-precursor ALL; *BCR-ABL* pos.					6.1	100
BE-13	T-lineage ALL					4.4	100
Jurkat	T-lineage ALL					6.1	100
KG-1a	AML					12.7	100
K562	CML, blast crisis					8.4	100
K562-r	K562, cytarabine-resistant					11.2	100

Patient number	Sex	Age	FAB	Cytogenetics	Molecular genetics	Clinical state	IC50 (µM)	Max. inhib. (%)
1	M	20	M5	46,XY	*FLT3*-ITD, *NPM1* mut.	R	5.7	100
2	F	71	M4	Complex karyotype[a]	*FLT3* wt, *NPM1* wt	N	7.1	96
3	M	40	M5	46,XY del(11)(p13~14p15)	*FLT3* wt, *NPM1* wt	R	7.6	95
4	M	70	M4	47,XY +8, t(11;19)	*FLT3* wt, *NPM1* wt	N	8.6	92
5	F	50	ND	46,XX	*FLT3* wt, *NPM1* wt	N	8.6	100
6	F	37	M4	46,XX	*FLT3*-ITD, *NPM1* wt	N	8.9	100
7	M	22	M5b	46,XY t(9;11)(p22;q23)	*FLT3*-ITD, *NPM1* wt	N	8.9	97
8	M	66	M4	47,XY + 8	*FLT3*-ITD, *NPM1* wt	N	9.0	88
9	F	43	M4	46,XX	*FLT3* wt, *NPM1* mut.	N	11.8	100
10	F	67	M2	46,XX	*FLT3* wt, *NPM1* wt	N	15.3	99
11	F	58	M1	46,XX	*FLT3*-ITD, *NPM1* wt	R	18.7	79
12	F	60	M5a	46,XX	*FLT3*-ITD, *NPM1* wt	N	37.2	82

Abbreviations: AML, acute myeloid leukemia; ALL, acute lymphoblastic leukemia; CML, chronic myeloid leukemia; FAB, French-American-British classification; PFT-µ, pifithrin-µ; M, male; F, female; Max., maximum; inh., inhibition; ITD, internal tandem duplication; ND, not defined; mut., mutated; wt, wild type; R, samples of relapsed AML; N, samples of newly diagnosed AML; WST-1, (2-[4-Iodophenyl]-3-[4-nitrophenyl]-5-[2,4-disulfophenyl]-2H-tetrazolium).
Cells were cultured in the presence of 0.5–100 µM PFT-µ for 48 h and viability was determined by WST-1 assay.
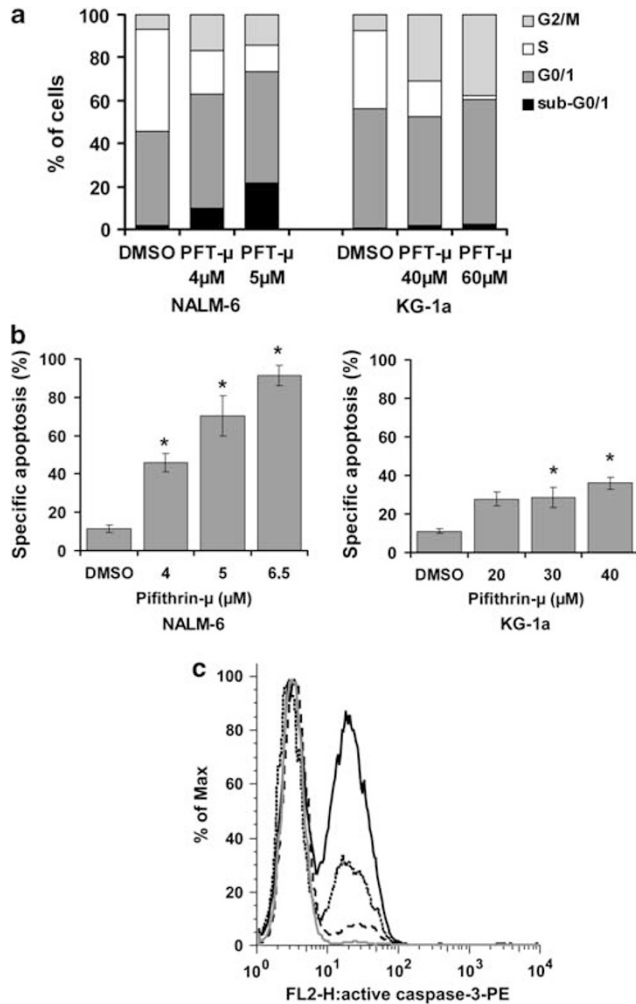[a]52,XX, +1, -3, del5 (q2?, 2q3?5), +11, +19, +21, -22, +4.

4

Figure 2 Cell cycle arrest, apoptosis and caspase-3 activation induced by PFT-μ in NALM-6 and KG-1a cells. (**a**) Cell cycle arrest after PFT-μ determined by BrdU/7-AAD staining and fluorescence-activated cell sorting analysis. A representative result is shown. Percent of cells in sub-G0/1, G0/1, S and G2/M phase, respectively. NALM-6 dimethyl sulfoxide control: 1.6, 44.1, 47.7, 6.6; NALM-6 4 μM PFT-μ: 9.9, 53.0, 20.3, 16.8; NALM-6 5 μM PFT-μ: 21.6, 51.8, 12.3, 14.3; KG-1a dimethyl sulfoxide control: 0.4, 55.8, 36.6, 7.2; KG-1a 40 μM PFT-μ: 1.7, 50.9, 16.2, 31.1; KG-1a 60 μM PFT-μ: 2.4, 58.0, 2.0, 37.6. (**b**) Dose-dependent induction of apoptosis by PFT-μ determined by AnnexinV/7-AAD staining and fluorescence-activated cell sorting analysis. Means of four values from three independent experiments plus standard errors are shown. The statistical significance between treated samples and dimethyl sulfoxide control was calculated by the Mann–Whitney U-test. *P<0.05. (**c**) Induction of activated caspase-3 by PFT-μ in NALM-6. NALM-6 cells were incubated with PFT-μ for 24 h, and activated caspase-3 was determined using a monoclonal anti-active-caspase-3 antibody and subsequent fluorescence-activated cell sorting analyses. Y-axis values of overlay histograms are normalized to % of maximum. Curves represent samples treated with dimethyl sulfoxide (grey), 3 μM PFT-μ (black dashed), 4 μM PFT-μ (black dotted) and 5 μM PFT-μ (black solid), showing 1%, 14%, 34% and 56% active caspase-3 positive cells, respectively.

about 22% of NALM-6 cells were in the sub-G0/1 fraction after incubation with 5 μM PFT-μ (two-fold IC50), whereas only 2% of KG-1a cells were observed within this fraction after 60 μM PFT-μ (4.7-fold IC50; Figure 2a).

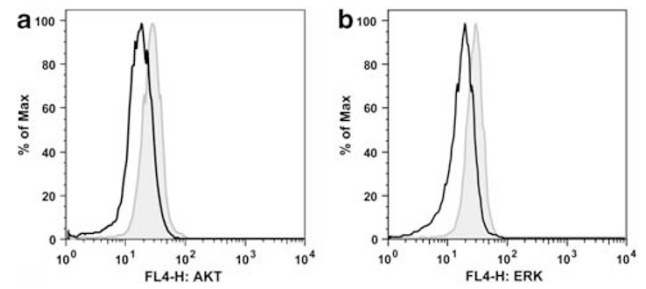The impact of PFT-μ on specific apoptosis was determined by AnnexinV/7–AAD staining after incubation with various

Figure 3 Impact of PFT-μ on intracellular AKT and ERK1/2 levels. NALM-6 cells were incubated with 10 μM PFT-μ for 10 h and concentrations of AKT and ERK1/2 proteins were measured with intracellular staining and fluorescence-activated cell sorting analyses. Representative figures are demonstrated. Grey line indicates dimethyl sulfoxide control, black line indicates sample treated with PFT-μ. Y-axis values of overlay histograms are normalized to % of maximum. Decrease of (**a**) AKT and (**b**) ERK1/2 following PFT-μ.

concentrations of PFT-μ for 48 h in NALM-6, KG-1a, TOM-1, BE-13, Jurkat and K562 cells. PFT-μ significantly induced specific apoptosis in all cell lines in a dose-dependent fashion (Figure 2b; data only shown for NALM-6 and KG-1a). In accordance with the results from cell cycle analyses, induction of apoptosis by PFT-μ was more pronounced in NALM-6 cells as compared with KG-1a. In NALM-6, incubation with PFT-μ at 4, 5 and 6.5 μM resulted in 34, 59 and 80% apoptotic cells above spontaneous apoptosis (11%), respectively. KG-1a cells showed a rate of specific apoptosis of 17% (20 μM PFT-μ), 18% (30 μM PFT-μ) and 25% (40 μM PFT-μ) above control (11%; Figure 2b).

Determination of caspase-3 activation revealed a dose-dependent increase of the cleaved, active form of caspase-3 in NALM-6 cells after treatment with 3, 4 and 5 μM PFT-μ for 24 h (Figure 2c). In KG-1a, no caspase-3 activation was detected after incubation with 20, 40 and 60 μM PFT-μ. This observation was further strengthened by the fact that pre-incubation with pan caspase inhibitor Z-VAD-FMK (50 μM for 1 h) significantly reduced apoptosis after PFT-μ in NALM-6, whereas KG-1a cells were not rescued by Z-VAD-FMK (data not shown). Thus, PFT-μ exerted different impacts on cell cycle and apoptosis in the two leukemic cell lineages.

PFT-μ reduces intracellular concentrations of AKT and ERK1/2 in NALM-6 cells
Next, we performed intracellular staining and fluorescence-activated cell sorting analyses of AKT, p-AKT, ERK1/2 and p-ERK1/2 kinases in NALM-6 cells to evaluate whether PFT-μ affects these two major signaling kinases or their phosphorylation status. After incubation with 10 μM PFT-μ for 10 h, a decrease in AKT and ERK1/2 levels was detected (Figure 3). Interestingly, concentrations of the phosphorylated forms p-AKT and p-ERK1/2 were very low at baseline and did not change after PFT-μ treatment (data not shown).

PFT-μ sensitizes acute leukemia cells to antileukemic drugs
To determine the potential use of combination therapy of PFT-μ with classic and novel antileukemic drugs, we performed co-incubation experiments of PFT-μ with HSP90 inhibitor 17-AAG, cytarabine, histone deacetylase inhibitor SAHA and multikinase inhibitor sorafenib in NALM-6, TOM-1 and KG-1a cells.

Combination of PFT-μ with 17-AAG resulted in a significantly decreased cell viability, compared with either drug alone. In detail, viability for PFT-μ and 17-AAG monotherapies in
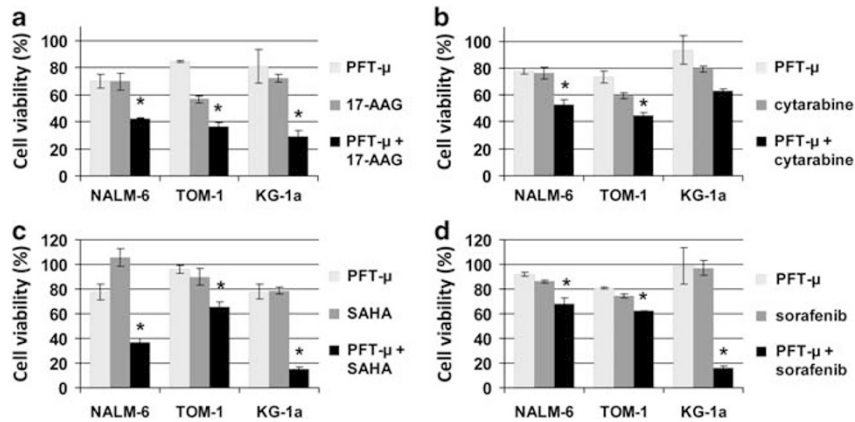
Figure 4 Antileukemic effect of combination of PFT-μ with 17-AAG, cytarabine, SAHA or sorafenib. Cells were co-incubated for 48 h and viability was measured by WST-1 assay. Means of at least four replicates plus standard errors of representative experiments are shown. The statistical significance between combination treatment and both single agents was calculated by the Mann–Whitney *U*-test. *P < 0.05. (**a**) Viability after incubation with PFT-μ and 17-AAG (NALM-6: 2 μM PFT-μ, 2 μM 17-AAG; TOM-1: 3 μM PFT-μ, 1 μM 17-AAG; KG-1a: 10 μM PFT-μ, 5 μM 17-AAG). (**b**) Viability after incubation with PFT-μ and cytarabine (NALM-6: 2 μM PFT-μ, 9 nM cytarabine; TOM-1: 3 μM PFT-μ, 40 nM cytarabine; KG-1a: 10 μM PFT-μ, 100 nM cytarabine). (**c**) Viability after incubation with PFT-μ and SAHA (NALM-6: 2 μM PFT-μ, 0.6 μM SAHA; TOM-1: 3 μM PFT-μ, 0.4 μM SAHA (given 24 h prior to PFT-μ); KG-1a: 25 μM PFT-μ, 0.4 μM SAHA (given 24 h prior to PFT-μ). (**d**) Viability after incubation with PFT-μ and sorafenib (NALM-6: 2 μM PFT-μ, 3 μM sorafenib; TOM-1: 3 μM PFT-μ, 4 μM sorafenib; KG-1a: 7 μM PFT-μ, 1 μM sorafenib).

comparison with combination treatment was 70%, 70% versus 42% in NALM-6 (2 μM PFT-μ, 2 μM 17-AAG), 85%, 57% versus 36% in TOM-1 (3 μM PFT-μ, 1 μM 17-AAG), and 81%, 72% versus 29% in KG-1a (10 μM PFT-μ, 5 μM 17-AAG), respectively (Figure 4a). Also, co-incubation of PFT-μ with cytarabine showed a decrease of cell proliferation, as compared with the particular monotherapy; cell viability of monotherapies versus combination were as follows: NALM-6 (2 μM PFT-μ, 9 nM cytarabine): 78%, 76% versus 53%; TOM-1 (3 μM PFT-μ, 40 nM cytarabine): 74%, 59% versus 45%; KG-1a (10 μM PFT-μ, 100 nM cytarabine): 93%, 80% versus 63% (Figure 4b). Combination of PFT-μ with SAHA induced significant additive effects regarding viability in all cell lines. Cell viability for either monotherapy at indicated concentrations versus combination treatment were 78%, 100% versus 37% for NALM-6 (2 μM PFT-μ, 6 μM SAHA), 96%, 90% versus 65% for TOM-1 (3 μM PFT-μ, 0.4 μM SAHA), and 78%, 79% versus 55% for KG-1a (25 μM PFT-μ, 0.4 μM SAHA; Figure 4c). Interestingly, combination of PFT-μ and SAHA in TOM-1 and KG-1a cells was most effective when SAHA was administered 24 h before PFT-μ as described in the methodical section. Simultaneous treatment of cells with PFT-μ and sorafenib resulted in a significant inhibition of proliferation with viability values for either substance, alone or the combination for NALM-6: 92%, 86% versus 68% (2 μM PFT-μ, 3 μM sorafenib), for TOM-1: 81%, 75% versus 62% (3 μM PFT-μ, 4 μM sorafenib), and for KG-1a: 99%, 97% versus 16% (7 μM PFT-μ, 1 μM sorafenib; Figure 4d). Thus, addition of PFT-μ increased the cytotoxic effect of all drugs tested both in myeloid and in lymphoblastic cell lines. Although KG-1a was the least sensitive cell line for PFT-μ as monotherapy, combination treatment of PFT-μ with 17-AAG, SAHA or sorafenib seemed most effective in this otherwise resistant cell line.[35]

Notably, combination of 17-AAG and SAHA with PFT-μ particularly revealed cytotoxic effects. As synergistic effects might be caused by upregulation of HSP70 secondary to drug exposure, HSP70 expression was determined by intracellular fluorescence-activated cell sorting analysis in NALM-6 cells after 18 h incubation. Treatment with 10 μM 17-AAG and treatment with 5 μM SAHA resulted in a significant upregulation of HSP70 protein (Figure 5). No impact of cytarabine or sorafenib on intracellular HSP70 concentration was seen (data
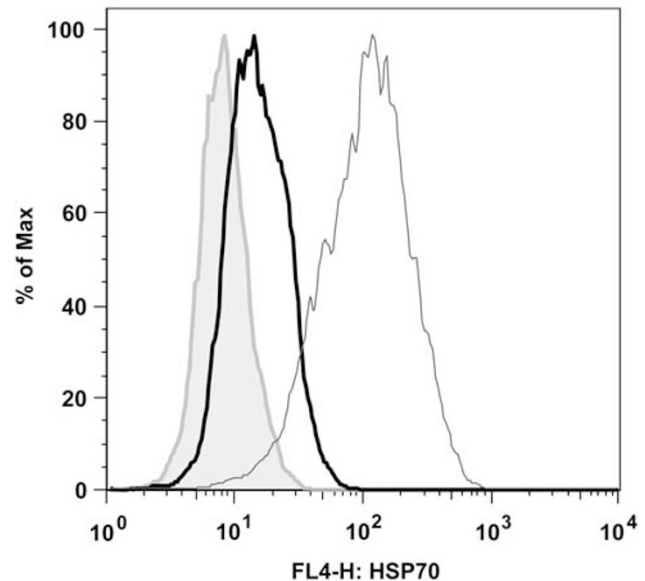

Figure 5 Induction of HSP70 by 17-AAG and SAHA in NALM-6 cells. NALM-6 cells were incubated with 10 μM 17-AAG or 5 μM SAHA for 18 h, and HSP70 levels were measured with intracellular staining and fluorescence-activated cell sorting analysis. A representative figure is shown. Grey line indicates dimethyl sulfoxide control, black thick line indicates sample treated with SAHA, black thin line indicates sample treated with 17-AAG. Y-axis values of overlay histograms are normalized to % of maximum.

not shown). Thus, the high antileukemic potential of PFT-μ in combination with 17-AAG or SAHA might be explained by the functional abrogation of HSP70 upregulation in response to these specific drugs.

Discussion

HSP70 provides a promising target for antileukemic therapy due to its aberrant expression, and its antiapoptotic and tumor-promoting effects in leukemic cells. Here, we describe for the

6

first time the potent *in vitro* effects of the HSP70 inhibitor PFT-μ in acute leukemias.

As we have shown, PFT-μ substantially inhibited cell viability already at low micromolar concentrations in a broad range of AML, T-ALL and B-precursor ALL cell lines (including *BCR-ABL* positive ALL). PFT-μ was also active in cytarabine-resistant K562 cells at only slightly higher IC50 values than in the cytarabine-sensitive parental cell line. Importantly, PFT-μ was highly effective in primary AML blasts with a median IC50 comparable with IC50 values of the cell lines tested. No significant association between patients' clinical and genetic characteristics and IC50 values of PFT-μ was seen in this small set of patient samples.

Normal hematopoietic cells and stromal cells revealed a markedly higher resistance to PFT-μ, as compared with primary leukemic blasts. Median IC50 value in BMSC was about fourfold higher, compared with leukemic blasts, with one BMSC sample not even reaching 50% inhibition of viability with 100 μM PFT-μ. In PB MNC and CD34-positive cells, median IC50 values for PFT-μ were about twofold higher, in comparison with primary AML blasts. These results suggest a limited BM toxicity of PFT-μ and underline the selective action of the inhibitor against neoplastic cells as described by Leu et al.[31] for solid tumors.

In leukemia cells, PFT-μ led to a remarkable loss of viability within a very narrow concentration range, unlike the shallow slope inhibition curve of classic cytostatic drugs. This phenomenon has previously been described for HSP90 inhibitors[34,36] and might be a class-specific effect of HSP inhibitors. The underlying cellular mechanisms are yet unknown.

We have further shown induction of cell cycle arrest and apoptosis by PFT-μ in acute leukemia cell lines. In both NALM-6 and KG-1a cells, a dose-dependent reduction of S-phase proliferating cells after PFT-μ exposure was demonstrated. The decrease in S phase was accompanied by a prominent increase of KG-1a cells in G2 arrest and a shift to both G0/1 and G2/M phase for NALM-6. Annexin V/7–AAD staining revealed a significant induction of specific apoptosis by PFT-μ in all cell lines tested; however, the effect was more pronounced in NALM-6 than in KG-1a cells. Interestingly, NALM-6 showed activation of caspase-3 after treatment with PFT-μ, whereas no increase in active caspase-3 could be detected in KG-1a.

The impact of HSP70 on control and regulation of caspase activity has been described before.[37] In the study of Leu et al.,[31] PFT-μ did not activate caspases in U2OS osteosarcoma cells, whereas another recent publication described caspase-induced cell death in chronic lymphatic leukemia cells by the inhibitor.[38] Our data further indicate that the individual effects of PFT-μ on cell cycle and caspase activation may be highly variable between different cancer cell lines, possibly due to a differential distribution and function of HSP70 isoforms as described for solid tumors by Powers et al.[22]

To further analyse the molecular effects of PFT-μ, we performed intracellular fluorescence-activated cell sorting analyses of the protein kinases AKT and ERK1/2 in NALM-6 cells. After incubation with PFT-μ, a decrease of intracellular AKT and ERK1/2 levels was detected. The stabilizing effects of HSP70 on AKT have been reported by Koren et al.[39] In their study, cytotoxic effects of HSP70 inhibition in breast cancer cell lines were restricted to cells with deregulated AKT function. As aberrantly activated PI3K/PTEN/AKT/mTOR and Raf/MEK/ERK1/2 pathways are the main promoters of leukemia cell survival,[40] degradation of the effector kinases AKT and ERK1/2 may be, in part, responsible for the antiproliferative and proapoptotic effects of PFT-μ seen in our study. Interestingly, levels of the phosphorylated proteins p-AKT and p-ERK1/2 were barely

detectable and remained unaffected by PFT-μ. Phosphorylated kinases are stabilized by HSP90, although the selective binding mechanism is unknown.[41] On the basis of our findings, combination of PFT-μ with HSP90 inhibitors could be synergistically effective by targeting both unphosphorylated and phosphorylated kinases.

To evaluate the cytotoxic effect of PFT-μ in combination with different antineoplastic drugs, we performed co-incubation proliferation assays with 17-AAG, cytarabine, SAHA and sorafenib. PFT-μ potently increased the inhibition of viability of all substances tested. However, the most prominent results were detected in the combinations with 17-AAG or SAHA. Synergistic effects of concomitant inhibition of HSP70 and HSP90 have been demonstrated before.[22,24,29] This is mainly attributed to a compensatory upregulation of HSP70 as a result of HSP90 inhibition. In accordance with previous studies,[42,43] we could demonstrate that both 17-AAG and SAHA treatment led to increased HSP70 levels in NALM-6 cells. Thus, functional abrogation of the HSP70 response induced by HSP90 and histone deacetylase inhibitors may explain the remarkable antiproliferative effects of PFT-μ in combination with SAHA and especially with 17-AAG.

In KG-1a cells, combination of PFT-μ and sorafenib was shown to be highly active. Overexpression of HSP70 has been associated with resistance to tyrosine kinase inhibitors.[28] Moreover, synergistic effects of HSP90 inhibitors with tyrosine kinase inhibitors have been described, even in early clinical studies.[44,45] Our findings further strengthen the promising sensitizing effect of HSP70 inhibitors in combination with sorafenib, which is already in clinical trials in AML.

Only few pharmacological inhibitors of HSP70 have been identified to date, with most of them lacking specificity or properties necessary for clinical use.[8,46] Just recently, PFT-μ has been described to specifically inhibit the inducible form of HSP70, without binding of HSP90.[31] Given the fact that Leu et al.[31] could show a reduced tumorigenicity in an Eμ-Myc-transgenic mouse model treated with PFT-μ over several weeks, the inhibitor seems to be applicable in an *in vivo* setting. However, further biochemical analyses have to be done in future studies to evaluate the exact mechanism of action of PFT-μ, as well as its pharmacological attributes.

In summary, we have demonstrated the potent *in vitro* effects of the HSP70 inhibitor PFT-μ in acute leukemia cell lines of lymphoid and myeloid origin, as well as in primary AML blasts. With respect to the sensitizing effects of PFT-μ for classic and novel cytotoxic agents, we consider the inhibitor an interesting candidate for further studies in acute leukemia.

Conflict of interest

The authors declare no conflict of interest.

Acknowledgements

References

1 Rowe JM, Tallman MS. How I treat acute myeloid leukemia. *Blood* 2010; **116**: 3147–3156.
2 Gökbuget N, Hoelzer D. Treatment of adult acute lymphoblastic leukemia. *Semin Hematol* 2009; **46**: 64–75.

3 Thomas DA. Philadelphia chromosome positive acute lymphocytic leukemia: a new era of challenges. *Hematology Am Soc Hematol Educ Program* 2007, 435–443.

4 Furukawa Y, Vu HA, Akutsu M, Odgerel T, Izumi T, Tsunoda S *et al*. Divergent cytotoxic effects of PKC412 in combination with conventional antileukemic agents in FLT3 mutation-positive versus -negative leukemia cell lines. *Leukemia* 2007; **21**: 1005–1014.

5 Cilloni D, Martinelli G, Messa F, Baccarani M, Saglio G. Nuclear factor κB as a target for new drug development in myeloid malignancies. *Haematologica* 2007; **92**: 1224–1229.

6 Golay J, Cuppini L, Leoni F, Mico C, Barbui V, Domenghini M *et al*. The histone deacetylase inhibitor ITF2357 has anti-leukemic activity *in vitro* and *in vivo* and inhibits IL-6 and VEGF production by stromal cells. *Leukemia* 2007; **21**: 1892–1900.

7 Lancet JE, Gojo I, Burton M, Quinn M, Tighe SM, Kersey K *et al*. Phase I study of the heat shock protein 90 inhibitor alvespimycin (KOS-1022, 17-DMAG) administered intravenously twice weekly to patients with acute myeloid leukemia. *Leukemia* 2010; **24**: 699–705.

8 Powers MV, Jones K, Barillari C, Westwood I, van Montfort RL, Workman P. Targeting HSP70: the second potentially druggable heat shock protein and molecular chaperone? *Cell Cycle* 2010; **9**: 1542–1550.

9 Mosser DD, Morimoto RI. Molecular chaperones and the stress of oncogenesis. *Oncogene* 2004; **23**: 2907–2918.

10 Jaattela M. Escaping cell death: survival proteins in cancer. *Exp Cell Res* 1999; **248**: 30–43.

11 Conroy SE, Latchman DS. Do heat shock proteins have a role in breast cancer? *Br J Cancer* 1996; **74**: 717–721.

12 Nanbu K, Konishi I, Mandai M, Kuroda H, Hamid AA, Komatsu T *et al*. Prognostic significance of heat shock proteins HSP70 and HSP90 in endometrial carcinomas. *Cancer Detect Prev* 1998; **22**: 549–555.

13 Thomas X, Campos L, Mounier C, Cornillon J, Flandrin P, Le QH *et al*. Expression of heat-shock proteins is associated with major adverse prognostic factors in acute myeloid leukemia. *Leuk Res* 2005; **29**: 1049–1058.

14 Steiner K, Graf M, Hecht K, Reif S, Rossbacher L, Pfister K *et al*. High HSP70-membrane expression on leukemic cells from patients with acute myeloid leukemia is associated with a worse prognosis. *Leukemia* 2006; **20**: 2076–2079.

15 Yeh CH, Tseng R, Hannah A, Estrov Z, Estey E, Kantarjian H *et al*. Clinical correlation of circulating heat shock protein 70 in acute leukemia. *Leuk Res* 2010; **34**: 605–609.

16 Volloch VZ, Sherman MY. Oncogenic potential of Hsp72. *Oncogene* 1999; **18**: 3648–3651.

17 Jaattela M. Over-expression of hsp70 confers tumorigenicity to mouse fibrosarcoma cells. *Int J Cancer* 1995; **60**: 689–693.

18 Seo JS, Park YM, Kim JI, Shim EH, Kim CW, Jang JJ *et al*. T cell lymphoma in transgenic mice expressing the human Hsp70 gene. *Biochem Biophys Res Commun* 1996; **218**: 582–587.

19 Jaattela M, Wissing D, Kokholm K, Kallunki T, Egeblad M. Hsp70 exerts its anti-apoptotic function downstream of caspase-3-like proteases. *Embo J* 1998; **17**: 6124–6134.

20 Nylandsted J, Brand K, Jaattela M. Heat shock protein 70 is required for the survival of cancer cells. *Ann NY Acad Sci* 2000; **926**: 122–125.

21 Rohde M, Daugaard M, Jensen MH, Helin K, Nylandsted J, Jaattela M. Members of the heat-shock protein 70 family promote cancer cell growth by distinct mechanisms. *Genes Dev* 2005; **19**: 570–582.

22 Powers MV, Clarke PA, Workman P. Dual targeting of HSC70 and HSP72 inhibits HSP90 function and induces tumor-specific apoptosis. *Cancer Cell* 2008; **14**: 250–262.

23 Schmitt E, Maingret L, Puig PE, Rerole AL, Ghiringhelli F, Hammann A *et al*. Heat shock protein 70 neutralization exerts potent antitumor effects in animal models of colon cancer and melanoma. *Cancer Res* 2006; **66**: 4191–4197.

24 Davenport EL, Zeisig A, Aronson LI, Moore HE, Hockley S, Gonzalez D *et al*. Targeting heat shock protein 72 enhances Hsp90 inhibitor-induced apoptosis in myeloma. *Leukemia* 2010; **24**: 1804–1807.

25 Kwak HJ, Jun CD, Pae HO, Yoo JC, Park YC, Choi BM *et al*. The role of inducible 70-kDa heat shock protein in cell cycle control, differentiation, and apoptotic cell death of the human myeloid leukemic HL-60 cells. *Cell Immunol* 1998; **187**: 1–12.

26 Creagh EM, Carmody RJ, Cotter TG. Heat shock protein 70 inhibits caspase-dependent and -independent apoptosis in Jurkat T cells. *Exp Cell Res* 2000; **257**: 58–66.

27 Guo F, Sigua C, Bali P, George P, Fiskus W, Scuto A *et al*. Mechanistic role of heat shock protein 70 in Bcr-Abl-mediated resistance to apoptosis in human acute leukemia cells. *Blood* 2005; **105**: 1246–1255.

28 Pocaly M, Lagarde V, Etienne G, Ribeil JA, Claverol S, Bonneu M *et al*. Overexpression of the heat-shock protein 70 is associated to imatinib resistance in chronic myeloid leukemia. *Leukemia* 2007; **21**: 93–101.

29 Guo F, Rocha K, Bali P, Pranpat M, Fiskus W, Boyapalle S *et al*. Abrogation of heat shock protein 70 induction as a strategy to increase antileukemia activity of heat shock protein 90 inhibitor 17-allylamino-demethoxy geldanamycin. *Cancer Res* 2005; **65**: 10536–10544.

30 Williamson DS, Borgognoni J, Clay A, Daniels Z, Dokurno P, Drysdale MJ *et al*. Novel adenosine-derived inhibitors of 70 kDa heat shock protein, discovered through structure-based design. *J Med Chem* 2009; **52**: 1510–1513.

31 Leu JI, Pimkina J, Frank A, Murphy ME, George DL. A small molecule inhibitor of inducible heat shock protein 70. *Mol Cell* 2009; **36**: 15–27.

32 Schmidt-Hieber M, Busse A, Reufi B, Knauf W, Thiel E, Blau IW. Bendamustine, but not fludarabine, exhibits a low stem cell toxicity *in vitro*. *J Cancer Res Clin Oncol* 2009; **135**: 227–234.

33 Blau O, Hofmann WK, Baldus CD, Thiel G, Serbent V, Schumann E *et al*. Chromosomal aberrations in bone marrow mesenchymal stroma cells from patients with myelodysplastic syndrome and acute myeloblastic leukemia. *Exp Hematol* 2007; **35**: 221–229.

34 Kaiser M, Lamottke B, Mieth M, Jensen MR, Quadt C, Garcia-Echeverria C *et al*. Synergistic action of the novel HSP90 inhibitor NVP-AUY922 with histone deacetylase inhibitors, melphalan, or doxorubicin in multiple myeloma. *Eur J Haematol* 2010; **84**: 337–344.

35 Fuchs D, Daniel V, Sadeghi M, Opelz G, Naujokat C. Salinomycin overcomes ABC transporter-mediated multidrug and apoptosis resistance in human leukemia stem cell-like KG-1a cells. *Biochem Biophys Res Commun* 2010; **394**: 1098–1104.

36 Stuhmer T, Zollinger A, Siegmund D, Chatterjee M, Grella E, Knop S *et al*. Signalling profile and antitumour activity of the novel Hsp90 inhibitor NVP-AUY922 in multiple myeloma. *Leukemia* 2008; **22**: 1604–1612.

37 Garrido C, Brunet M, Didelot C, Zermati Y, Schmitt E, Kroemer G. Heat shock proteins 27 and 70: anti-apoptotic proteins with tumorigenic properties. *Cell Cycle* 2006; **5**: 2592–2601.

38 Steele AJ, Prentice AG, Hoffbrand AV, Yogashangary BC, Hart SM, Lowdell MW *et al*. 2-Phenylacetylenesulfonamide (PAS) induces p53-independent apoptotic killing of B-chronic lymphocytic leukemia (CLL) cells. *Blood* 2009; **114**: 1217–1225.

39 Koren III J, Jinwal UK, Jin Y, O'Leary J, Jones JR, Johnson AG *et al*. Facilitating Akt clearance via manipulation of Hsp70 activity and levels. *J Biol Chem* 2010; **285**: 2498–2505.

40 Steelman LS, Abrams SL, Whelan J, Bertrand FE, Ludwig DE, Basecke J *et al*. Contributions of the Raf/MEK/ERK, PI3K/PTEN/Akt/mTOR and Jak/STAT pathways to leukemia. *Leukemia* 2008; **22**: 686–707.

41 Pearl LH, Prodromou C, Workman P. The Hsp90 molecular chaperone: an open and shut case for treatment. *Biochem J* 2008; **410**: 439–453.

42 Marinova Z, Ren M, Wendland JR, Leng Y, Liang MH, Yasuda S *et al*. Valproic acid induces functional heat-shock protein 70 via Class I histone deacetylase inhibition in cortical neurons: a potential role of Sp1 acetylation. *J Neurochem* 2009; **111**: 976–987.

43 Jensen H, Andresen L, Hansen KA, Skov S. Cell-surface expression of Hsp70 on hematopoietic cancer cells after inhibition of HDAC activity. *J Leukoc Biol* 2009; **86**: 923–932.

44 George P, Bali P, Cohen P, Tao J, Guo F, Sigua C *et al*. Cotreatment with 17-allylamino-demethoxygeldanamycin and FLT-3 kinase inhibitor PKC412 is highly effective against human acute myelogenous leukemia cells with mutant FLT-3. *Cancer Res* 2004; **64**: 3645–3652.

45 Vaishampayan UN, Burger AM, Sausville EA, Heilbrun LK, Li J, Horiba MN *et al*. Safety, efficacy, pharmacokinetics, and pharmacodynamics of the combination of sorafenib and tanespimycin. *Clin Cancer Res* 2010; **16**: 3795–3804.

46 Jego G, Hazoume A, Seigneuric R, Garrido C. Targeting heat shock proteins in cancer. *Cancer Lett* 2010; e-pub ahead of print 13 November 2010; doi:10.1016/j.canlet.2010.10.014.